

# VUV spectroscopy of $\text{Tm}^{3+}$ and $\text{Mn}^{2+}$ doped $\text{LiSrAlF}_6$

M. True\*, M. Kirm, E. Negodine, S. Vielhauer, G. Zimmerer

*Institut für Experimentalphysik, University of Hamburg, Hamburg, Germany*

## Abstract

$\text{LiSrAlF}_6$  (LiSAF) crystals doped with either  $\text{Tm}^{3+}$  or  $\text{Mn}^{2+}$  were obtained by solid-state reaction and investigated spectroscopically using synchrotron radiation in the vacuum-ultra-violet and ultra-violet spectral regions. In the  $\text{Tm}^{3+}$  doped LiSAF crystals, the slow spin-forbidden 5d–4f emission peaking at 166 nm with a lifetime of at least 1  $\mu\text{s}$  was observed. The respective excitation spectrum consists of several bands in the range of 160–110 nm arising due to the 4f–5d absorption. The f–f emissions of  $\text{Tm}^{3+}$  are well excited in the range of 135–110 nm, but not under excitation into the lower lying d-bands. The excitation mechanisms of different emissions will be discussed including the  $\text{F}^-$  to  $\text{Tm}^{3+}$  charge transfer excitation peaking at 127 nm in LiSAF. The characteristic broad  ${}^4\text{T}_1 \rightarrow {}^6\text{A}_1$  emission band of  $\text{Mn}^{2+}$  peaking at 508 (504) nm was observed in LiSAF: $\text{Mn}^{2+}$  crystal at 10 (300) K. Three intense excitation bands, tentatively ascribed to the 3d–4s transitions of  $\text{Mn}^{2+}$ , were revealed in the range of 170–110 nm.

© 2003 Elsevier B.V. All rights reserved.

*Keywords:* Insulators; Fluorides; Rare earth ions; Luminescence; Synchrotron radiation

## 1. Introduction

Due to numerous applications as solid-state lasers in the ultra-violet wavelength region [1] or optical elements for lithography using 157 nm lasers [2], the properties of  $\text{LiCaAlF}_6$  (LiCAF) and the isostructural  $\text{LiSrAlF}_6$  (LiSAF) crystals have been investigated. LiCAF is found to be very stable concerning the creation of X-ray induced colour centres as well as the gradual surface damage in air [3]. LiCAF and LiSAF crystals are transparent up to 112 and 116 nm, respectively [4]. This makes them promising candidates as hosts for phosphors in mercury free discharge lamps, converting the broad Xenon discharge emission (172 nm) into visible photons with quantum efficiency higher than unity [5]. LiSAF has a trigonal structure with lattice parameters  $a = 0.508$  nm and  $c = 1.021$  nm [6]. For doping it offers the octahedral  $\text{Sr}^{2+}$  and  $\text{Al}^{3+}$  lattice sites.

This motivates the investigation of  $\text{Tm}^{3+}$  ions doped into LiSAF crystals, providing strong spin-allowed f–d absorption in the vacuum-ultra-violet (VUV) and f–f emission in the UV-Vis range. Except for  ${}^1\text{S}_0$ , the 4f-levels cover the range up to  $\sim 34\,500$   $\text{cm}^{-1}$  and are well separated from the d-levels at considerably higher energy. Emission from the highest f-state,  ${}^1\text{S}_0$ , located above  $75\,000$   $\text{cm}^{-1}$  within

the d-levels has not been observed yet. Pappalardo showed that if exciting only the f-levels high quantum efficiency cannot be achieved in fluorides singly doped with  $\text{Tm}^{3+}$  [7].

$\text{Mn}^{2+}$  is evaluated as a candidate for co-doping to achieve efficient down conversion of the absorbed energy in the VUV range.  $\text{Mn}^{2+}$  is widely used in phosphors as strong emitter in the visible. The energy levels of the 3d<sup>5</sup> states depend strongly on the crystal field. Excitation into the higher d-states relaxes non-radiatively to the first excited state ( ${}^4\text{T}_1$ ) with subsequent broad emission to the ground state ( ${}^6\text{A}_1$ ). Thus, inter-ionic energy transfer between rare earth ions and  $\text{Mn}^{2+}$  is a prospective possibility. However,  $\text{Mn}^{2+}$  excitation or absorption in the VUV range has been hardly investigated. This work comprises a characterisation of LiSAF: $\text{Tm}^{3+}$  and LiSAF: $\text{Mn}^{2+}$  with the main focus on the VUV range.

## 2. Experimental

LiSAF: $\text{Tm}^{3+}$  and LiSAF: $\text{Mn}^{2+}$  were prepared by the solid-state reaction method at the Institute of Laser Physics (University of Hamburg). A stoichiometric mixture of highly pure (99.99%) LiF,  $\text{SrF}_2$ , and  $\text{AlF}_3$  powders were used with 1% of the  $\text{Sr}^{2+}$  ions substituted by the dopant.  $\text{Sr}^{2+}$  was substituted by  $\text{Li}^+$  in the same amount as  $\text{Tm}^{3+}$  in order to maintain charge neutrality. The mixed powders were fired at 850 °C in HF enriched nitrogen atmosphere to remove

\* Corresponding author.

E-mail address: marcus.true@desy.de (M. True).

residual oxygen [8], and then slowly cooled below the melting point of LiSAF (765 °C) within 12 h. This treatment resulted in large, transparent crystalline domains, which have been confirmed to be single phase LiSAF by X-ray diffraction analysis.

The crystals were characterised using time-resolved luminescence spectroscopy at the SUPERLUMI setup of HASYLAB at DESY under synchrotron radiation in the range of 330–50 nm with excitation pulses every 200 ns [9]. UV and visible emission was detected by photomultiplier (Hamamatsu R6358P) in conjunction with a spectrograph (Acton SpectraPro 308i). VUV emission was detected by a solar-blind photomultiplier (Hamamatsu R6836) with a 0.5 m Pouey-type VUV monochromator. The emission spectra were not corrected for the spectral response of the system. The excitation spectra were corrected for the incident photon flux. The crystals were cleaved in air just before mounting on a copper sample holder attached to a flow-type He cryostat. The temperature could be varied in the range of 10–300 K.

### 3. Results and discussion

The inset of Fig. 1 shows the emission spectra of LiSAF:Mn<sup>2+</sup> at 10 and 300 K excited at 127 nm. The broad luminescence of LiSAF:Mn<sup>2+</sup> peaking at 508 nm at 10 K corresponds to the lowest intra-shell <sup>4</sup>T<sub>1</sub> → <sup>6</sup>A<sub>1</sub> transition which is parity and spin-forbidden. In addition, a broad non-elementary emission band (250–450 nm) of the host crystal is observed under interband excitation. This is due to the radiative decay of self-trapped excitons and radiative recombination of electron-hole pairs at various centres discussed elsewhere for LiCAF [10]. This emission is completely quenched at 300 K, while the band due to the <sup>4</sup>T<sub>1</sub> → <sup>6</sup>A<sub>1</sub> transition is broadened

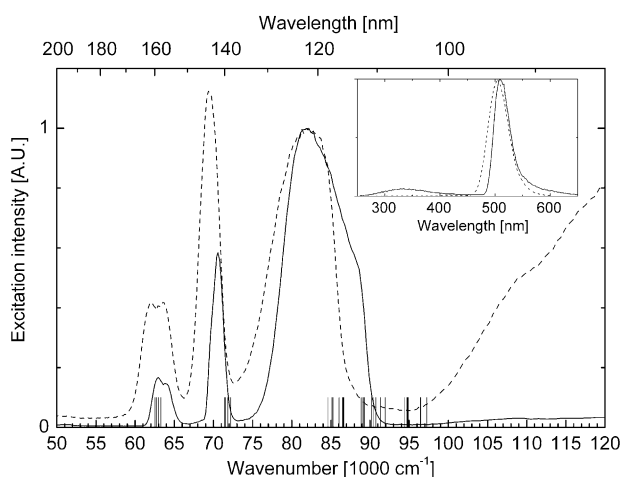


Fig. 1. Excitation spectra of LiSAF:Mn<sup>2+</sup> 515 nm emission at 10 (—) and 300 K (---). The 4s states of Mn<sup>2+</sup> free ion are indicated as horizontal lines. Inset: emission spectra excited at 127 nm (78 740 cm<sup>-1</sup>) at 10 K (—) and 300 K (---). The spectral resolution is 0.3 nm for excitation and 10 nm for emission.

and the peak is blue-shifted to 504 nm. Monitoring this emission, the excitation spectrum shown in Fig. 1 reveals three strong bands in the VUV region. At 300 K their maxima are located at 62 900 cm<sup>-1</sup> (FWHM 4400 cm<sup>-1</sup>), 69 500 (2900), and 81 800 (8900), while at 10 K they were recorded at 63 500 cm<sup>-1</sup> (2600 cm<sup>-1</sup>), 70 600 (1900), and 82 200 (10 000). Similar results were also obtained from LiCAF:Mn<sup>2+</sup>, where the excitation bands are slightly blue-shifted compared with LiSAF:Mn<sup>2+</sup> [11], in agreement with the higher field depression of LiCAF [12]. Analogous bands with comparable peak positions and widths have been detected in the absorption spectra of Mn<sup>2+</sup> doped fluorides and were assigned to intra-ionic 3d–4s transitions [13]. One could think of 3d–3d transitions in the energy region above 60 000 cm<sup>-1</sup> as well. However, since no bands with comparable intensity were detected below 60 000 cm<sup>-1</sup>, we tentatively ascribe the excitation bands in VUV to the 3d–4s transitions in the Mn<sup>2+</sup> ion. The respective energy level data for free Mn<sup>2+</sup> ions supports our interpretation; the <sup>6</sup>D and <sup>4</sup>D multiplets of the 3d4s configuration have their barycentres at 62 800 and 71 700 cm<sup>-1</sup> [14].

Excitation into the host above 98 000 cm<sup>-1</sup> causes the formation of electron-hole pairs leading to efficient Mn<sup>2+</sup> emission in LiSAF:Mn<sup>2+</sup>, while at 10 K this process is less pronounced. The energy transfer by electron-hole pairs is responsible for the excitation of Mn<sup>2+</sup> centres at 300 K, but the transfer is less efficient at 10 K and the absorbed energy is mainly released via host emission.

If the Mn<sup>2+</sup> ion is substituted into a lattice site with octahedral symmetry, orange-red emission is typically expected due to the large crystal field, while in tetrahedral surroundings with a much smaller field the emission is usually green [15,16]. However, if the Mn<sup>2+</sup> ion is situated on a considerably larger lattice site, a lower crystal field is expected resulting in a shift of the emission towards higher energy, observed in crystals like SrB<sub>6</sub>O<sub>10</sub>:Mn<sup>2+</sup> with emission at 512 nm [17] and in GdF<sub>3</sub>:Mn<sup>2+</sup> with emission at 520 nm [18]. In our case the Al<sup>3+</sup> lattice site is considerably smaller (ionic radius 67 pm) compared to Mn<sup>2+</sup> (81 pm), while the Sr<sup>2+</sup> (130 pm) site is much larger. Both the Al<sup>3+</sup> and Sr<sup>2+</sup> lattice sites have octahedral symmetry. Nevertheless, green emission is detected for LiSAF:Mn<sup>2+</sup> at 508 nm. This confirms that Mn<sup>2+</sup> is incorporated on the Sr<sup>2+</sup> site.

In Fig. 2, 5d–4f emission of LiSAF:Tm<sup>3+</sup> at 10 K is presented, exciting into the higher d-states at 78 740 cm<sup>-1</sup> (127 nm). The most intense emission band at 166 nm arises due to the transition from the 5d to 4f ground state <sup>3</sup>H<sub>6</sub> and is followed by weaker transitions populating 4f-states up to <sup>3</sup>F<sub>2,3</sub>. The decay time of the emission is at least 1 μs, too slow to be measured accurately at our setup with an inter-pulse period of 200 ns. This confirms that only the slow spin-forbidden 5d–4f transition of Tm<sup>3+</sup> is observed as in KYF<sub>4</sub>:Tm<sup>3+</sup> at 168 nm [19].

Fig. 3 presents the emission spectra of LiSAF:Tm<sup>3+</sup> at 10 K in the UV-Vis range. Interband excitation at 125 000 cm<sup>-1</sup> (80 nm) results in a broad intrinsic emission

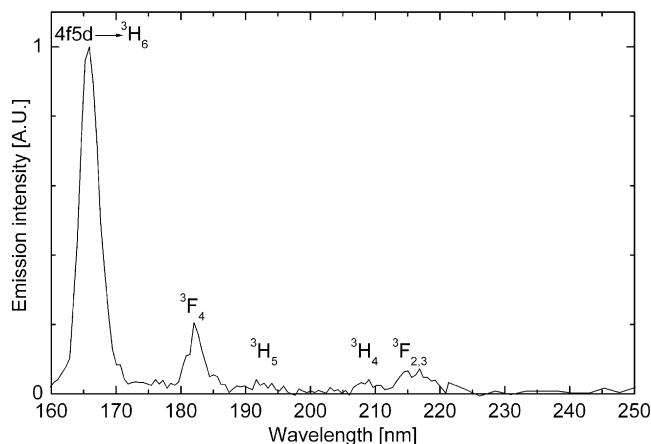


Fig. 2. Emission spectrum of LiSAF:Tm<sup>3+</sup> at 10 K, excited at 127 nm (78 740 cm<sup>-1</sup>). The spectral resolution is 2 nm.

band (upper part) of the same origin as discussed for LiSAF:Mn<sup>2+</sup>. This emission overlaps with the 4f absorption of Tm<sup>3+</sup> in the range of the <sup>1</sup>D<sub>2</sub> and (<sup>3</sup>P<sub>j</sub>, <sup>1</sup>I<sub>6</sub>) states, resulting in energy transfer and subsequent f–f emission observed as weak peaks at 455 and 485 nm.

Emission spectra excited at 86 200 (116 nm) and 78 740 cm<sup>-1</sup> (127 nm) are presented in the lower part of Fig. 3. The peaks are assigned to f–f transitions as indicated in the figure. If exciting with photons of lower energy, emissions starting from the <sup>1</sup>I<sub>6</sub> state are enhanced with respect to those arising from the <sup>1</sup>D<sub>2</sub> state. This is in agreement with the behavior of the respective excitation spectra in Fig. 4, indicating that several energy transfer processes occur populating f-levels in a different way.

Fig. 4 shows excitation spectra for various emissions of LiSAF:Tm<sup>3+</sup> at 9 K. Curve e shows the excitation for the spin-forbidden 5d–4f emission at 165.5 nm. The first strong band above 63 000 cm<sup>-1</sup> is due to the 4f–5d excitation into the low-spin state (spin-allowed transition). The 5d–4f luminescence is well excited in the lower d-bands

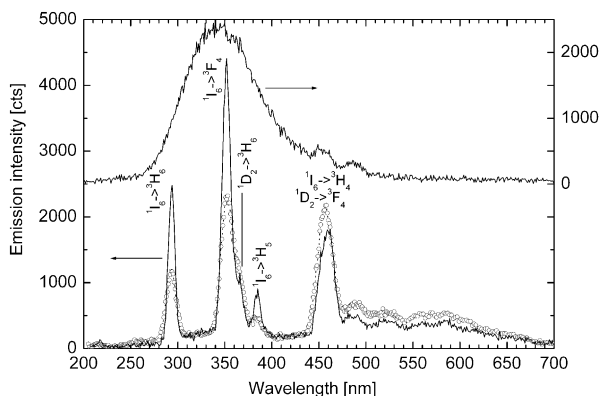


Fig. 3. Emission spectra of LiSAF:Tm<sup>3+</sup> at 9 K. Upper part: excited at 80 nm. Lower part: excited at 116 nm (○) and 127 nm (—). The intra-configurational 4f–4f transitions are assigned in the figure, assuming that <sup>1</sup>I<sub>6</sub> is the state with the lowest energy within the (<sup>3</sup>P<sub>j</sub>, <sup>1</sup>I<sub>6</sub>) mani-fold [26]. The spectral resolution is 5 nm for emission.

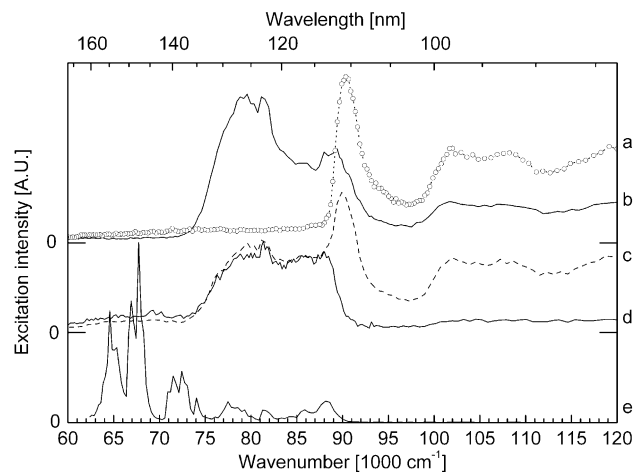


Fig. 4. Excitation spectra of LiSAF:Tm<sup>3+</sup> at 9 K for emissions detected at (a) 320 nm, (b) 293 nm, (c) 363 nm, (d) 455 nm, (e) 165.5 nm. The spectral resolution is 0.3 nm for excitation, 20 nm (curve a), and 10 nm (curves b–d) for emission. VUV emission (curve e) was recorded with a resolution of 3 nm.

(62 000–75 000 cm<sup>-1</sup>) with decreasing intensity in the upper d-bands (75 000–90 000 cm<sup>-1</sup>). No d–f luminescence is observed at higher excitation energies up to 110 000 cm<sup>-1</sup>.

The excitation of the broad-band host emission at 320 nm (curve a) reaches its maximum at 91 000 cm<sup>-1</sup>, ascribed to host exciton excitation. The intensity increase of the 320 nm host emission as well as of Mn<sup>2+</sup> luminescence (Fig. 1) above 98 000 cm<sup>-1</sup> suggests that creation of free electron-hole pairs occurs, corresponding to the energy gap in LiSAF.

In order to analyse the population mechanisms of <sup>1</sup>I<sub>6</sub> and <sup>1</sup>D<sub>2</sub>, the respective wavelengths for transitions to the ground state <sup>3</sup>H<sub>6</sub> were chosen, i.e. 293 nm (curve b) and 363 nm (curve c). The efficient excitation of the Tm<sup>3+</sup> f–f transitions in LiSAF at 10 K starts above 74 000 cm<sup>-1</sup>. The excitonic peak and host excitation observed in these spectra are due to the overlap with the broad-band host emission, while this is not the case for the emission at 455 nm (curve d), which comprises both <sup>1</sup>I<sub>6</sub> → <sup>3</sup>H<sub>6</sub> and <sup>1</sup>D<sub>2</sub> → <sup>3</sup>F<sub>4</sub> emissions.

The efficient excitation of f–f emissions in VUV raises the question for the underlying process. Following VUV excitation, the emission of more than one photon can be achieved by either photon cascade emission within one ion like in Pr<sup>3+</sup> [7] or a cross-relaxation process populating the lower lying state of two different ions [20]. Such cross-relaxations play a role already at rather low doping concentration as shown for LiYF<sub>4</sub>:Er [21]. Excitation into the higher d-states of Tm<sup>3+</sup> is followed by the rapid non-radiative relaxation to the lowest d-state (62 000 cm<sup>-1</sup>), which can serve as initial state for cross-relaxation and radiative decay. However, since f–f emissions are efficiently excited only above 74 000 cm<sup>-1</sup>, cross-relaxation can be excluded. Also a radiative cascade starting from the 5d state can be excluded for the same reason. Moreover, according to Fig. 3, the 5d–4f emission populates only the states up to <sup>3</sup>F<sub>2,3</sub>.

Since the onset of the 4f-emissions is in the region where no strong d-absorption is observed, it has to originate from a different excitation process. The charge transfer (CT) from anion to cation is well-established manifesting as separate excitation band in  $\text{Eu}^{3+}$  doped fluorides [22]. For other rare earth ions the CT excitation bands overlap with the f–d bands and the assignment is based mostly on theoretical estimates available for fluorides and oxides [23]. Dorenbos has shown that the position of d-levels can be predicted with high accuracy relative to the position for  $\text{Ce}^{3+}$  in the same host [11,24]. A similar approach is feasible for predicting CT transitions, if the corresponding  $\text{Eu}^{3+}$  CT state is known [25]. According to our unpublished measurements the maximum of the CT excitation band in LiCAF:Eu crystals is located at  $65\,300\text{ cm}^{-1}$ ; the respective  $\text{F}^- \rightarrow \text{Tm}^{3+}$  CT transition in LiCAF is expected  $13\,470\text{ cm}^{-1}$  higher in energy [25]. In analogy, the excitation band of f–f emissions peaking at  $79\,000\text{ cm}^{-1}$  is ascribed to CT absorption, populating the higher lying f-states ( $^1\text{I}_6$ ,  $^3\text{P}_1$ ) non-radiatively as confirmed by the respective emission spectrum in Fig. 3. The d-states are bypassed in this process.

The excitation efficiency of transitions starting from  $^1\text{D}_2$  is practically the same in the energy range of  $78\,000\text{--}90\,000\text{ cm}^{-1}$ . At photon energies approaching the host absorption the  $^1\text{D}_2$  state becomes presumably populated via radiative transfer from emission centres of extrinsic origin. In LiCAF as well in LiSAF the broad-band emission arising from the radiative decay of near impurity excitons and impurity/defect centres is shifted to the longer wavelengths, which provides better overlap with lower lying f-states.

In this work, the luminescence of LiSAF: $\text{Tm}^{3+}$  and LiSAF: $\text{Mn}^{2+}$  doped crystals under VUV excitation was investigated. The intra-centre excitation bands were found for both ions in the transparency range of LiSAF. The d-f luminescence of  $\text{Tm}^{3+}$  is excited via the respective f–d absorption, while several excitation channels exist for f–f emissions.

## Acknowledgements

This work was supported by the BMBF Verbund-Projekt “VUV-Leuchtstoffe für effiziente quecksilberfreie Entla-

ungslampen” no. 03N8019D. We would like to thank P. Dorenbos for helpful discussions and sharing the unpublished data. The help of D. Schiffbauer is gratefully acknowledged in providing the X-ray diffraction analysis.

## References

- [1] C.D. Marshall, J.A. Speth, S.A. Payne, W.F. Krupke, G.J. Quarles, V. Castillo, B.H.T. Chai, *J. Opt. Soc. Am. B* 11 (1994) 2054.
- [2] E. Sarantopoulou, Z. Kollia, A.C. Cefalas, *Opt. Comm.* 177 (2000) 377.
- [3] H. Sato, K. Shimamura, A. Bensalah, N. Solovieva, A. Beiterova, A. Vedda, M. Martini, H. Machida, T. Fukuda, M. Nikl, *Jpn. J. Appl. Phys.* 41 (2002) 2028.
- [4] K. Shimamura, S.L. Baldochi, N. Mujilat, K. Nakano, Z. Liu, H. Othake, N. Sarukura, T. Fukuda, *J. Cryst. Growth* 211 (2000) 302.
- [5] S. Kück, I. Sokolska, *J. Electrochem. Soc.* 149 (2002) J27.
- [6] V.W. Viebahn, *Z. Anorg. Allg. Chem.* 386 (1971) 335.
- [7] R. Pappalardo, *J. Lumin.* 14 (1976) 159.
- [8] R.F. Belt, R. Uhrin, *J. Cryst. Growth* 109 (1991) 340.
- [9] G. Zimmerer, *Nucl. Instr. Meth. A* 308 (1991) 178.
- [10] N.V. Shiran, A.V. Gektin, S.V. Neicheva, V.A. Kornienko, K. Shimamura, N. Ishinose, *J. Lumin.* 102/103 (2003) 815.
- [11] M. True, M. Kirm, G. Zimmerer, to be published.
- [12] P. Dorenbos, *J. Lumin.* 91 (2000) 155.
- [13] J.F. Sabatini, A.E. Salwin, D.S. McClure, *Phys. Rev. B* 11 (1975) 3832.
- [14] NIST Atomic Spectra Database. <http://www.nist.gov/srd/>.
- [15] D.T. Palumbo, J.J. Brown Jr., *J. Electrochem. Soc.* 117 (1970) 1184.
- [16] D.T. Palumbo, J.J. Brown Jr., *J. Electrochem. Soc.* 118 (1971) 1159.
- [17] T. Koskentalo, M. Leskelä, L. Niinistö, *Mater. Res. Bull.* 20 (1985) 265.
- [18] S.H.M. Poort, A. Meijerink, G. Blasse, *Sol. State Comm.* 103 (1997) 537.
- [19] N.M. Khaidukov, M. Kirm, S.K. Lam, D. Lo, V.N. Makhov, G. Zimmerer, *Opt. Com.* 184 (2000) 183.
- [20] R.T. Wegh, H. Donker, K.D. Oskam, A. Meijerink, *Science* 283 (1999) 663.
- [21] N.M. Khaidukov, N.Yu. Kirikova, M. Kirm, J.C. Krupa, V.N. Makhov, E. Negodin, G. Zimmerer, *Proc. SPIE* 4766 (2002) 154.
- [22] I. Gérard, J.C. Krupa, E. Simoni, P. Martin, *J. Alloys Comp.* 207/208 (1994) 120.
- [23] A.N. Belsky, J.C. Krupa, *Displays* 19 (1999) 185.
- [24] P. Dorenbos, *J. Lumin.* 91 (2000) 91.
- [25] P. Dorenbos, *J. Phys.: Condens. Matter* 15 (2003) 8417.
- [26] J.B. Gruber, M.E. Hills, R.M. Macfarlane, C.A. Morrison, G.A. Turner, G.J. Quarles, G.J. Kintz, L. Esterowitz, *Phys. Rev. B* 40 (1989) 9464.